

Structural and magnetic properties of epitaxial Heusler alloy $\text{Fe}_2\text{Cr}_{0.5}\text{Co}_{0.5}\text{Si}$

Yu-Pu Wang, Gu-Chang Han, Hui Lu, Jinjun Qiu, Qi-Jia Yap, and Kie-Leong Teo

Citation: *Journal of Applied Physics* **115**, 17C301 (2014); doi: 10.1063/1.4852117

View online: <http://dx.doi.org/10.1063/1.4852117>

View Table of Contents: <http://scitation.aip.org/content/aip/journal/jap/115/17?ver=pdfcov>

Published by the [AIP Publishing](#)

Articles you may be interested in

[Tunnel magnetoresistance effect in magnetic tunnel junctions using Fermi-level-tuned epitaxial \$\text{Fe}_2\text{Cr}_{1-x}\text{Co}_x\text{Si}\$ Heusler alloy](#)

J. Appl. Phys. **115**, 17C709 (2014); 10.1063/1.4862720

[Epitaxial films of Heusler compound \$\text{Co}_2\text{FeAl}_{0.5}\text{Si}_{0.5}\$ with high crystalline quality grown by off-axis sputtering](#)

Appl. Phys. Lett. **103**, 162404 (2013); 10.1063/1.4825338

[Phase separation in \$\text{Fe}_2\text{CrSi}\$ thin films](#)

J. Appl. Phys. **114**, 113908 (2013); 10.1063/1.4821972

[Tunnel magnetoresistance effect and interface study in magnetic tunnel junctions using epitaxial \$\text{Fe}_2\text{CrSi}\$ Heusler alloy electrode](#)

J. Appl. Phys. **114**, 013910 (2013); 10.1063/1.4812725

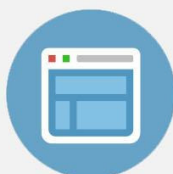
[High tunnel magnetoresistance in fully epitaxial magnetic tunnel junctions with a full-Heusler alloy \$\text{Co}_{2-x}\text{Cr}_x\text{Fe}_{0.4}\text{Al}_{0.6}\$ thin film](#)

Appl. Phys. Lett. **88**, 262503 (2006); 10.1063/1.2217166



Re-register for Table of Content Alerts

Create a profile.



Sign up today!



Structural and magnetic properties of epitaxial Heusler alloy $\text{Fe}_2\text{Cr}_{0.5}\text{Co}_{0.5}\text{Si}$

Yu-Pu Wang,^{1,2,a)} Gu-Chang Han,² Hui Lu,¹ Jinjun Qiu,² Qi-Jia Yap,² and Kie-Leong Teo¹

¹Department of Electrical and Computer Engineering, National University of Singapore, 4 Engineering Drive 3, Singapore 117583

²Data Storage Institute, Agency for Science, Technology and Research (A*STAR), 5 Engineering Drive 1, Singapore 117608

(Presented 7 November 2013; received 12 September 2013; accepted 1 October 2013; published online 2 January 2014)

This paper reports the study of structural and magnetic properties of Heusler alloy $\text{Fe}_2\text{Cr}_{0.5}\text{Co}_{0.5}\text{Si}$ (FCCS) thin film and its tunnel magnetoresistance (TMR) effect. The smooth quaternary Heusler alloy FCCS film with surface roughness of rms value of 0.25 nm measured by atomic force microscopy and partial $L2_1$ phase was obtained by magnetron sputtering at room temperature followed by *in-situ* annealing at 400 °C. The saturation magnetization and coercivity of FCCS are 410 emu/cm³ and 20 Oe, respectively. The magnetic tunnel junctions (MTJs) using FCCS as free layer were studied in detail as a function of post-annealing temperature. A TMR ratio of 15.6% has been achieved with 300 °C post-annealing. This is about twice the highest TMR ratio obtained in MTJs using Fe_2CrSi . The enhancement of TMR ratio can be attributed to the successful tuning of the Fermi level of Fe_2CrSi close to the center of the minority band gap by Co-doping.
 © 2014 AIP Publishing LLC. [<http://dx.doi.org/10.1063/1.4852117>]

Half-metallic ferromagnets (HMFs) with only electrons of one spin at Fermi level (E_F) are desired in spintronics devices such as magnetic tunnel junctions (MTJs) as it can provide 100% spin polarized current.¹ Full Heusler alloys are promising candidates of HMFs, which belong to a group of ternary intermetallic compounds of general formula X_2YZ with a $L2_1$ structure. It can be described by means of four interpenetration fcc lattices and characterized by the positions X_1 ($1/4, 1/4, 1/4$), X_2 ($3/4, 3/4, 3/4$), Y (000), and Z ($1/2, 1/2, 1/2$). The half metallicity of Heusler alloy is fragile against atomic disorder. When the Y and Z atoms swap their sites and eventually occupy their sites absolutely at random, the $L2_1$ structure transforms into the $B2$ structure. In addition, X - Y and X - Z disorder finally form the $A2$ structure.²

Full-Heusler alloy Fe_2CrSi (FCS) has been predicted to be a HMF with low magnetization ($2 \mu_B/\text{f.u.}$) and reasonable Curie temperature (~ 630 K).^{3,4} This temperature is low enough for thermally assisted switching and yet high enough compared to the room temperature (RT). However, MTJs using $B2$ phase FCS as the bottom electrode have yielded a low tunnel magnetoresistance (TMR) ratio ($\sim 8.1\%$) at RT.⁵ One of the reasons is that the density of states (DOS) of majority spin of FCS at E_F is very sharp and the E_F is close to the band edge of minority spin. Hence, the spin polarization of FCS may be strongly reduced by thermal fluctuation. Recent theoretical study⁶ has shown that robust half metallicity as well as high TMR ratio would be expected in Co-doped FCS such as $\text{Fe}_2\text{Cr}_{0.5}\text{Co}_{0.5}\text{Si}$ (FCCS) due to the shift of E_F close to the center of the minority band gap.

In this work, we have achieved FCCS thin film with partial $L2_1$ phase which has a better chemical ordering than $B2$ phase FCS. The MTJs using FCCS as free layer were studied in detail as a function of post-annealing temperature (T_{pa}).

The highest TMR ratio measured at RT is 15.6% for MTJs with $T_{pa} = 300$ °C, which is about 2 times larger than that using FCS.

A single layer of FCCS (30 nm) was deposited on MgO (100) substrate with a Cr (40 nm) buffer layer and capped with Ru (3 nm). All films were deposited at RT and then *in-situ* annealed at various temperatures (T_{ia}) in an ultra-high vacuum magnetron sputtering system with base pressure of 10^{-7} Pa. The T_{ia} is 600 °C for MgO substrates, 700 °C for Cr buffer layer, and 350 °C \sim 450 °C for FCCS thin film. After optimizing the growth conditions of FCCS film, MTJs with Cr (40 nm)/FCCS (30 nm)/Mg (0.3 nm)/MgO (0.7 nm)/CoFe (3 nm)/IrMn (8 nm)/Ru (3 nm) were fabricated. The *ex-situ* post-annealed at various T_{pa} ranging from 235 °C to 400 °C were carried out in high vacuum in the presence of an in-plane magnetic field of 1 Tesla in order to develop an exchange bias (EB) between CoFe and IrMn layers. The Mg insertion layer is used to prevent the oxidation of FCCS by MgO barrier during MgO deposition and subsequent post annealing.⁵

Figure 1(a) shows the X-ray diffraction patterns of MgO substrate/Cr (40 nm)/FCCS (30 nm)/Ru (3 nm) under various T_{ia} . The epitaxial relation is MgO (001) [100]/Cr (001) [110]/FCCS (001) [110]. The MgO (200) and Cr (200) peaks are detected in all films indicating [100]-preferred orientation. The FCCS (200) and (400) peaks are observed with $T_{ia} = 400$ °C and 450 °C indicating that the ordering of FCCS thin films transfers from $A2$ to $B2$ or $L2_1$. The peak intensity is higher for $T_{ia} = 450$ °C. The lattice constants of FCCS under $T_{ia} = 400$ °C and 450 °C estimated from the 2θ scans are 5.590 ± 0.005 Å and 5.630 ± 0.005 Å, respectively. These values are close to the calculated lattice constant of 5.649 Å.⁷ Furthermore, the full-width-at-half-maximum (FWHM) of the diffraction peak in rocking curve measurements of FCCS (400) peak are 0.8° and 0.6° for $T_{ia} = 400$ °C and 450 °C, respectively, as compared to the value of 1.3° reported in

^{a)}Electronic mail: wangyupu@nus.edu.sg.

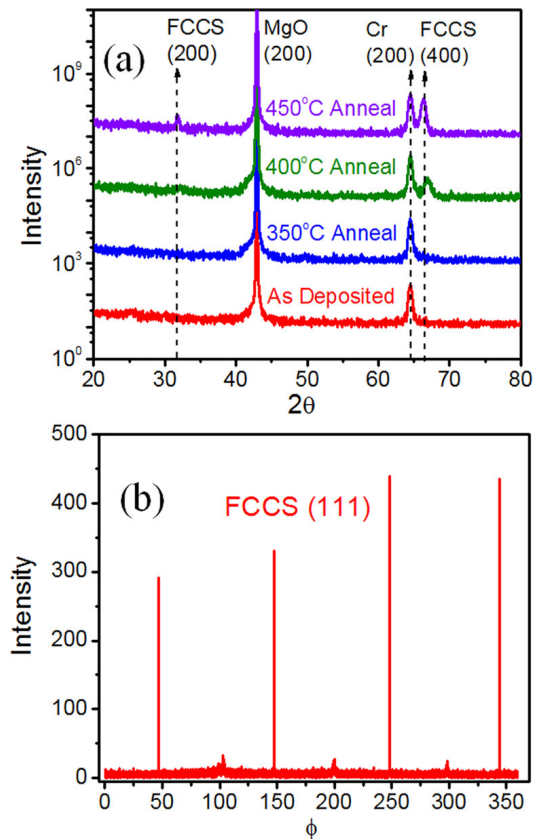


FIG. 1. (a) X-ray diffraction patterns for FCCS thin films under various annealing temperatures. From bottom to top: as deposited, $T_{ia} = 350^\circ\text{C}$, 400°C , and 450°C , respectively; (b) ϕ scan of FCCS (111) peak for sample with $T_{ia} = 400^\circ\text{C}$.

Ref. 4. Although $T_{ia} = 450^\circ\text{C}$ gives rise to a better FCCS crystalline structure, the rms value of 0.47 ± 0.02 nm measured by atomic force microscopy is too rough for MTJs, since the MgO barrier layer in MTJs is typically only 1 nm thick. The rough bottom electrode layer may cause the formation of pinholes in such a thin MgO barrier which will suppress the TMR effect. This is similar to that previously reported in Ref. 4 in which the films deposited at high temperatures show rough surfaces. The best rms value is $\sim 0.25 \pm 0.01$ nm obtained at $T_{ia} = 400^\circ\text{C}$. We have also investigated the [111] orientation of the films by the in plane ϕ -scan to confirm the $L2_1$ ordering of the FCCS films. As shown in Fig. 1(b), the diffraction peaks from the (111) superlattice reflection, which corresponds to $L2_1$ structure, are observed for FCCS film at $T_{ia} = 400^\circ\text{C}$. This indicates the existence of $L2_1$ phase in our FCCS film. Since $L2_1$ phase in FCCS has a better chemical ordering than $B2$ phase FCS, higher spin polarization as well as higher TMR ratio would be expected.

Figure 2(a) depicts the saturation magnetization (M_S) and coercivity (H_C) of FCCS as a function of T_{ia} measured by alternating gradient magnetometer. The M_S of FCCS increases with the T_{ia} . In particular, there is a big increase of M_S value from 103 emu/cm^3 at $T_{ia} = 350^\circ\text{C}$ to 410 emu/cm^3 at $T_{ia} = 400^\circ\text{C}$. This can be attributed to the increase in ordering and better crystallization as demonstrated by XRD results in Fig. 1. Meanwhile, H_C decreases from 150 Oe to 5 Oe with increasing T_{ia} . The decrease in H_C can be explained by a possible reduction in defect density accompanied with an enhancement of crystalline quality. Figure 2(b)

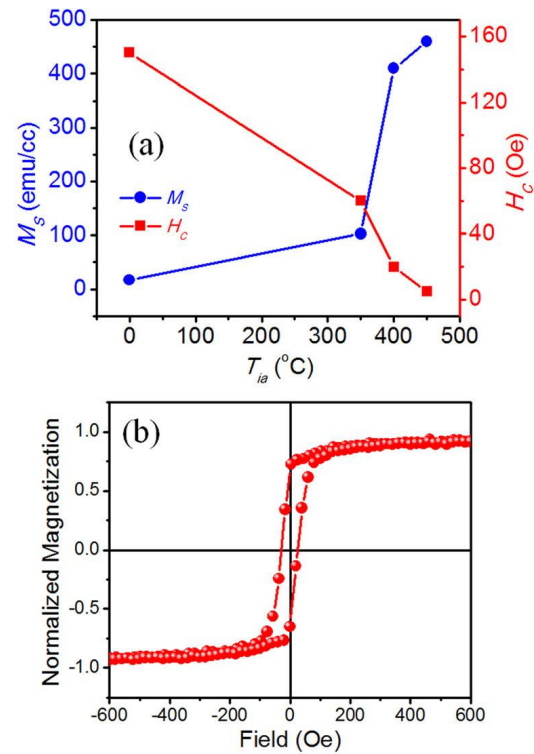


FIG. 2. (a) The T_{ia} dependence of M_S and H_C of FCCS; (b) M - H loop for FCCS with $T_{ia} = 400^\circ\text{C}$.

presents the M - H loop of FCCS with $T_{ia} = 400^\circ\text{C}$. The field was applied along the in-plane [011] direction, which is parallel to the easy axis of the crystalline anisotropy of FCCS. The value of H_C is 20 Oe, which is suitable for free layer in MTJ. The ratio of remnant magnetization (M_r) to M_S is 0.84, which indicates the magnetic easy-axis is along [011] direction. The M_S of FCCS is slightly larger than that of FCS ($\sim 398 \text{ emu/cm}^3$) due to Co substitution of Cr, but still smaller than that of Co_2MnSi , Co_2FeSi and Co_2FeAl ($1000 \sim 1200 \text{ emu/cm}^3$). The relatively low M_S of FCCS is favorable for low switching current density required for spin-transfer torque devices, such as Spin Transfer Torque Magnetoresistive Random Access Memory (STT-MRAM).⁸

As discussed above, the *in-situ* annealing at $T_{ia} = 400^\circ\text{C}$ gives the best FCCS performance for MTJ application. Therefore, T_{ia} is fixed at 400°C for FCCS layer in MTJs in the subsequent study. We have investigated the post-annealing effect ranging from $T_{pa} = 235^\circ\text{C}$ to 400°C . The EB is observed even without post-annealing as shown in Fig. 3(a). The switching field for the free layer and pinned layer is well separated with a shift of 352 Oe. The EB is better defined than that of FCS reported in Refs. 4 and 5. With $T_{pa} = 300^\circ\text{C}$, the EB still exists and the ratio of M_r to M_S (top hysteresis loop) increases, indicating a sharp magnetization reversal as shown in Fig. 3(a). However, when T_{pa} increases further, the ratio of M_r to M_S decreases (top hysteresis loop), signifying the degrading of crystalline structure of the top electrode. Finally, at $T_{pa} = 400^\circ\text{C}$, the EB is destroyed and the magnetization of free layer and pinned layer switch simultaneously. This could be due to the diffusion of Mn from IrMn into other layers.

The TMR effect was studied by Capres current-in-plane-tunneling technique⁹ on un-patterned MTJs at RT. The T_{pa} dependence of resistance-area product (RA) and TMR

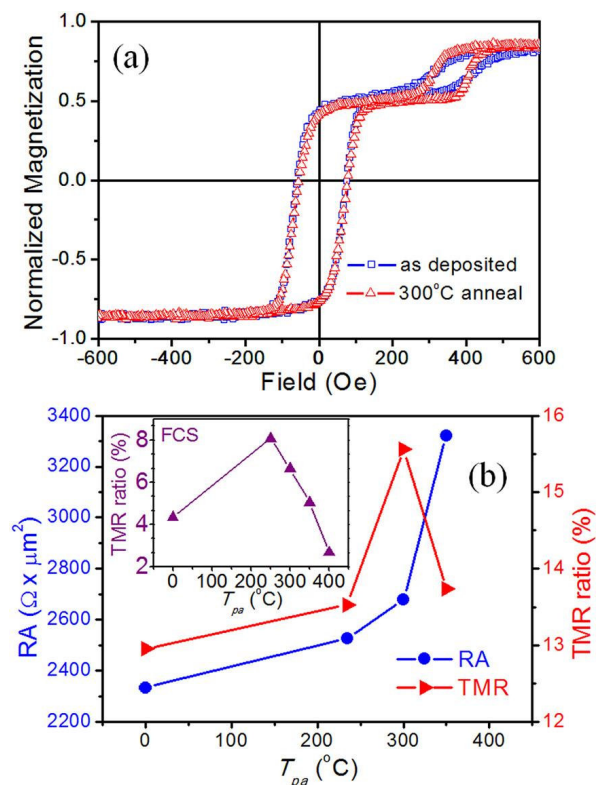


FIG. 3. (a) M - H loop for MTJs using FCCS as deposited (opened square) and $T_{pa}=300^\circ\text{C}$ (opened triangle); (b) RA and TMR ratio as functions of T_{pa} for MTJs using FCCS. The inset of (b) is the TMR ratio as a function of T_{pa} for MTJs using Fe₂CrSi.

ratio are shown in Fig. 3(b). The RA increases gradually with T_{pa} . This is most likely due to a better crystalline quality of MgO barrier after the post-annealing and oxygen diffusion to the bottom electrode. The TMR ratio initially increases with T_{pa} , then decreases after $T_{pa}=300^\circ\text{C}$ and finally vanishes at $T_{pa}=400^\circ\text{C}$. The highest TMR ratio of 15.6% is achieved at $T_{pa}=300^\circ\text{C}$. The highest TMR ratio is achieved with the compromise of the interface properties, the crystalline structure of MgO barrier and top electrode CoFe in post annealing process. The decrease and finally vanishing of TMR ratio can be attributed to the oxidation of FCCS at the interface and Mn diffusion from IrMn layer to other layers. The inset of Fig. 3(b) shows the TMR ratio as a function of T_{pa} for MTJs using FCS as bottom free layer, which has the same stack structure as the MTJs using FCCS. The highest TMR ratio of MTJs using FCS is 8.1% with $T_{pa}=250^\circ\text{C}$, which is only half of the value obtained with MTJs using FCCS at $T_{pa}=300^\circ\text{C}$. The higher TMR ratio in MTJs using FCCS could be due to the successful shifting of E_F position in FCCS close to the centre of minority gap as compared to FCS and the better $L2_1$ ordering in FCCS than in FCS. Our results are consistent with the theoretical calculation in Ref. 6. The higher T_{pa} for maximum TMR ratio can be ascribed to the sharper interface between MgO barrier and bottom free layer as well as better anti-oxidation of FCCS as compared to FCS.

We note that the TMR ratio achieved in our MTJs is still lower than the expected value from first-principle calculation.¹⁰ There are some possible reasons leading to the suppression of TMR ratio. First, the electronic and atomic structures of the ferromagnet/insulator interfaces play a

critical role in spin-dependent tunnelling in MTJs. A small variations in atomic potentials and bonding near the interface have a very strong effect on the interface DOS and on the conductance. The existence of interface states and their contribution to the tunneling current depend on the degree of hybridization between the orbitals on metal and insulator atoms. Variations in the atomic potentials and bonding strength near the interfaces have a profound effect resulting in the formation of interface resonant states. This dramatically affects the spin polarization and TMR.¹¹ In our previous study, we have shown that the insertion of an Mg layer of 0.3 nm thick can effectively prevent the oxidation of the bottom electrode by MgO barrier,⁵ resulting in significant enhancement of TMR ratio. However, we cannot confirm whether there is residual Mg or partial oxidation of FCCS along the whole interface. Therefore, by modifying the electronic properties of the interfaces and eliminating interface states, it is possible to enhance the TMR ratio. Second, the improvement of FCCS chemical ordering is another way to increase TMR ratio. Although our study shows that FCCS with $T_{ia}=450^\circ\text{C}$ has a better chemical ordering, the surface roughness of this sample is too large for MTJ application. Last but not the least, by adjusting the Co composition in Fe₂Cr_{1-x}Co_xSi, we can optimize the tuning of E_F to the center of minority band gap, thereby enhancing the TMR ratio.

In summary, single crystalline FCCS thin film with partial $L2_1$ phase is achieved by sputtering, which has better chemical ordering as compared to $B2$ phase FCS. The MTJ structure utilizing FCCS as the bottom free layer is fabricated and a TMR ratio of 15.6% is obtained after 300°C post-annealing. The higher TMR ratio and better thermal stability of FCCS as compared to FCS can be attributed to the shifting of E_F close to the center of minority band gap and the appearance of $L2_1$ ordering. For future work, we propose to improve the quality of ferromagnet/insulator interface and tune the E_F closer to the center of minority band gap by adjusting the Co composition in Fe₂Cr_{1-x}Co_xSi.

This work was supported by Singapore Agency for Science, Technology and Research (A*STAR), under Grant No. 092-151-0087.

¹R. A. de Groot, F. M. Mueller, P. G. van Engen, and K. H. J. Buschow, *Phys. Rev. Lett.* **50**, 2024 (1983).

²P. J. Webster and K. R. A. Ziebeck, "Heusler alloys," in Landolt-Börnstein New Series Group III Vol. 19C, edited by H. R. J. Wijn (Springer, Berlin, 1988), p. 75.

³H. Z. Luo, Z. Y. Zhu, L. Ma, S. F. Xu, H. Y. Liu, J. P. Qu, Y. X. Li, and G. H. Wu, *J. Phys. D: Appl. Phys.* **40**, 7121 (2007).

⁴S. Yoshimura, H. Asano, Y. Nakamura, K. Yamaji, Y. Takeda, M. Matsui, S. Ishida, Y. Nozaki, and K. Matsuyama, *J. Appl. Phys.* **103**, 07D716 (2008).

⁵Y. P. Wang, G. C. Han, H. Lu, J. J. Qiu, Q. J. Yap, R. Ji, and K. L. Teo, *J. Appl. Phys.* **114**, 013910 (2013).

⁶Y. Du, G. Z. Xu, E. K. Liu, G. J. Li, H. G. Zhang, S. Y. Yu, W. H. Wang, and G. H. Wu, *J. Magn. Magn. Mater.* **335**, 101 (2013).

⁷H. X. Luo, F. B. Meng, Y. Q. Cai, W. W. Hong, E. K. Liu, G. H. Wu, X. X. Zhu, and C. B. Jiang, *J. Magn. Magn. Mater.* **323**, 2323 (2011).

⁸S. Mangin, Y. Henry, D. Ravelosona, J. A. Katine, and E. E. Fullerton, *Appl. Phys. Lett.* **94**, 012502 (2009).

⁹D. C. Worledge and P. L. Trouilloun, *Appl. Phys. Lett.* **83**, 84 (2003).

¹⁰S. Fujii, S. Ishida, and S. Asano, *J. Phys. Soc. Jpn.* **81**, 034716 (2012).

¹¹E. Y. Tsybal, K. D. Belashchenko, J. P. Velev, S. S. Jaswal, M. van Schifgaarde, I. I. Oleynik, and D. A. Stewart, *Prog. Mater. Sci.* **52**, 401 (2007).